Comparison of methods for discontinuity roughness evaluation

Anna Maria Ferrero,* Maria Rita Migliazza,** Gessica Umili*

Summary

Rock masses are natural media affected by the presence of discontinuities that influence significantly their stability conditions: blocks are detached by the discontinuity planes and can move along them; moreover, the possible kinematisms are ruled by the amount of shear strength offered by the discontinuities. Shear strength depends on mechanical properties but also on geometrical aspects of a discontinuity, such as its roughness. For this reason, the evaluation of this property is fundamental. In this paper the state of the art of the roughness descriptors is presented. The two surfaces of a joint, digitalized by means of a photogrammetric survey and already used to perform shear tests (Ferrero *et al*., 2010], are used to apply the geometrical descriptors and analyze the results in terms of correspondence with laboratory results. Moreover, the influence of anisotropy and sampling interval (SI) is discussed. The paper compares different roughness quantitative descriptors showing as Tatone and Grasselli's approach [2011; 2013] is in good agreement with experimental shear tests data.

Introduction

Rock masses are natural media affected by the presence of discontinuities that influence significantly their stability conditions: blocks are detached by the discontinuity planes and can move along them; moreover, the possible kinematic motion are ruled by the amount of shear strength offered by the discontinuity. Shear strength depends on mechanical properties but also on geometrical aspects of a discontinuity, such as its roughness. For this reason the evaluation of this property is fundamental.

In the case of rough or non-planar joints, a non-linear shear strength envelope may be more representative of the test results [Muralha *et al.,* 2014]: two well-established failure criteria are the i value of Patton [Barton, 1976] and the JRC of Barton and Choubey [1977]. Most of the time the JRC value of a rock joint is estimated by visually comparing it to the ten standard profiles, with JRC values ranging from 0 to 20. In rock engineering practice, however, the visual comparison has been long thought to be subjective, since the user has to judge which profile his joint fits the best [Li and Zhang, 2015]. The development of objective methods for a quantitative estimation of JRC has been the research topic of many authors in recent years: regression correlations between JRC and geometrical, fractal, and geostatistical descriptors were proposed. Research was also focused on significant aspects that influence roughness quantitative estimate, such as the anisotropy of the discontinuity surface, the scale effect and the sampling interval (SI).

In this paper the state of the art of the roughness descriptors is presented. The two surfaces of a joint, digitalized by means of a photogrammetric survey and already used to perform shear tests [Ferrero *et al.,* 2010], are used to apply the geometrical descriptors and analyze the results in terms of correspondence with laboratory results. Moreover, the influence of anisotropy and SI are discussed.

1. State of the art of roughness assessment

A large number of methods to quantify joint surface roughness are described in the literature; for engineering purposes the Joint Roughness Coefficient (JRC) [Barton, 1973] is the most common: it varies from 0, for a smooth surface, to 20, for a very rough surface. JRC can be related to the results of tilt tests [Barton and Choubey, 1977] and therefore to shear strength. 10 standard roughness profiles have been used for a long time for visually comparing a

* Dipartimento di Scienze della Terra, Università degli Studi di Torino, Torino
** Dipartimento di Ingegneria Strutturale, Edile e Geotecnica, Politecnico di Torino, Torino

 DOI:10.19199/2019.2.0557-1405.008

natural profile and assigning a JRC value to it; in recent years this operation has been gradually substituted by manual digitization, laser profilometer and, more recently, by photogrammetric and laser scanner techniques, which allow for the acquisition of the whole surface of a discontinuity sample and therefore lead to the development of methods for determining both 2D and 3D roughness parameters.

In the following paragraphs a brief review of the main methods for assessing roughness and their evolution is reported.

2. Geometrical descriptors

Many statistical descriptors based on the geometry of rock joints profiles have been developed to quantitatively determine joint roughness: hereinafter the main ones and the authors who proposed empirical formulations to correlate them with JRC are listed.

– Root mean square roughness (RMS) [MYERS, 1962; TSE and CRUDEN, 1979]

$$RMS=\left(\frac{1}{M}\sum_{i=1}^{N-1} y_i^2 \Delta s\right)^{1/2} \quad (1)$$

where M is the number of sampling intervals, N the number of evenly spaced sampling points, y_i the height of the profile corresponding to the i-th sampling point, Δs the SI.

– Root mean square of the first derivative (Z_2) method [MYERS, 1962; TSE and CRUDEN, 1979; YU and VAYSSADE, 1991; YANG *et al.*, 2001]

$$Z_2=\left(\frac{1}{L}\sum_{i=1}^{N-1}\frac{(y_{i+1}-y_i)^2}{x_{i+1}-x_i}\right)^{1/2} \quad (2)$$

where L is the projected length of the profile and x_i is the abscissa of the i-th sampling point.

– Structural equation (SF) method (the mean square of the first derivative of the profile) [SAYLES and THOMAS, 1977; TSE and CRUDEN, 1979; YU and VAYSSADE, 1991; YANG *et al.*, 2001]

$$SF=\frac{1}{L}\sum_{i=1}^{N-1}(y_{i+1}-y_i)^2\,\Delta s=(Z_2\cdot\Delta s)^2 \quad (3)$$

Roughness profile index (R_P) method [EL-SOUDANI, 1978; MAERZ *et al.*, 1990; YU and VAYSSADE, 1991; TATONE and GRASSELLI, 2010] and its 3D analogous, R_S

$$R_P=\frac{\sum_{i=1}^{N-1}\sqrt{(x_{i+1}-x_i)^2+(y_{i+1}-y_i)^2}}{\sum_{i=1}^{N-1}(x_{i+1}-x_i)} \quad (4)$$

$$R_S=\frac{A_t}{A_n} \quad (5)$$

where A_t is the true surface area and A_n is the nominal surface area.

Maximum apparent asperity inclination (θ^*_{max}) method for 2D and 3D analysis [TATONE and GRASSELLI, 2010]

$$L_{\Theta^*}=L_0\left(\frac{\Theta^*_{MAX}-\Theta^*}{\Theta^*_{MAX}}\right)^C \quad (6)$$

$$A_{\Theta^*}=A_0\left(\frac{\theta^*_{MAX}-\theta^*}{\theta^*_{MAX}}\right)^C \quad (7)$$

where L_0 and A_0 are the normalized length and normalized area corresponding to $\theta^* = 0°$, respectively, θ^*_{max} is the inclination of the steepest segment or facet; and C is a dimensionless fitting parameter, calculated via a non-linear least-squares regression analysis, which characterizes the shape of the cumulative distribution [GRASSELLI *et al.*, 2002].

Many authors proposed correlations for deriving JRC from the above mentioned geometrical descriptors. The most commonly used are listed below:

$$JRC=32.2+32.47\cdot Log_{10}(Z_2)$$ TSE and CRUDEN [1979] (8)

$$JRC=37.28+16.58\cdot Log_{10}(SF)$$ TSE and CRUDEN [1979] (9)

$$JRC=32.69+32.98\cdot Log_{10}(Z_2)$$ YANG *et al.* [2001] (10)

$$JRC=37.63+16.5\cdot Log_{10}(SF)$$ YANG *et al.* [2001] (11)

$$JRC=51.85(Z_2)^{0.60}-10.37\ (SI=0.5\ mm)$$
TATONE and GRASSELLI [2010] (12)

$$JRC=55.03(Z_2)^{0.74}-6.10\ (SI=1.0\ mm)$$
TATONE and GRASSELLI [2010] (13)

$$JRC=3.95\left(\frac{\theta^*_{max}}{[C+1]_{2D}}\right)^{0.7}-7.98\ (SI=0.5\ mm)$$
TATONE and GRASSELLI [2010] (14)

$$JRC=2.40\left(\frac{\theta^*_{max}}{[C+1]_{2D}}\right)^{0.85}-4.42\ (SI=1.0\ mm)$$
TATONE and GRASSELLI [2010] (15)

A complete review of all the proposed empirical formulations can be found in LI and ZHANG [2015].

3. Fractal descriptors

Fractal geometry was originally introduced by MANDELBROT [1983] for describing irregular geometrical shapes. Fractals can be divided in two groups: self-similar and self-affine. MANDELBROT [1985] and KULATILAKE and UM [1997] suggested to use self-affine fractal models for joint roughness; ODLING [1994] states that the main ability of these models

is to predict the relationship between surface geometry observed at different scales. Fractal parameters can be estimated with different methods, such as divider (also called compass-walking), box counting, variogram, spectral, roughness-length and line scaling (see references in GE *et al.*, 2014].

Fractal dimension (D) has a minimum value of 1 for a perfectly smooth profile; Jiang et al. [2006] state that, since the real fractal dimension for a rock joint surface is between 2 and 3, three-dimensional fractal measurement, which considers the roughness surface as a whole, is required. Numerous empirical equations were put forward for estimating JRC using D: a complete review can be found in LI and HUANG [2015].

4. Geostatistical descriptors

The geostatistical tool utilized for describing the joint roughness profile is the variogram, defined as [JOURNEL and HUIJBREGTS, 1978] the expectation of the squared difference of two irregularity heights separated by a distance h:

$$2\gamma(x, h) = E[(z(x) - z(x + h))^2] \qquad (16)$$

where E denotes the expectation, x a geometrical position and z(x) the roughness height in x. Many authors proposed methods based on variograms to determine JRC, such as CARR [1990], FERRERO and GIANI [1990], KULATILAKE *et al.* [1998]. Particular contributions concerning the use of variograms were made by BELEM *et al.* [1997], who used variomaps (variance maps of the mean square height difference of points on the surface) to represent joint surface roughness, and by ROKO *et al.* [1997], who characterized the anisotropy of joint surface roughness. CHEN *et al.* [2016] used variogram in order to estimate the joint equivalent hydraulic aperture according to the sill and the range of the variogram.

5. Back-analysis of experimental tests

Back-analysis of JRC value is based on Barton's criterion [1973]:

$$JRC = \frac{\left(arctan\frac{\tau_p}{\sigma_n} - \emptyset_r\right)}{log_{10}\left(\frac{JCS}{\sigma_n}\right)} \qquad (17)$$

Shear tests should be performed on rock joints with different normal stress values, in order to obtain different pairs (σ_n, τ_p). The residual friction angle ϕ_r can be estimated from [BARTON and CHOUBEY, 1977]:

$$\phi_r = (\phi_b - 20) + 20\frac{r}{R} \qquad (18)$$

where ϕ_b is the basic friction angle, r and R are the Schmidt rebound number on a wet and weathered surface and on a dry unweathered sawn surface, respectively. ϕ_b should be evaluated on an artificially planar slickenside surface and it is characteristic of the rock mineralogy [GIANI, 1992]. Joint wall compressive strength (JCS) can be estimated following ISRM [1978].

6. Significant aspects: anisotropy, scale effect and SI

Rock discontinuities can be considered as failure surfaces due to physical or mechanical processes of fracturing cutting continuously through rock bodies [MANDL, 2005]. In particular, considering them as the result of mechanical processes, it is possible to assume that the evolution of the stress state could have influenced not only their orientation, spacing and persistence, but also the roughness of the breakage surfaces. Roughness depends also on the microstructure of the rock (type, crystals dimension, level of cementation and connection) and on the kind of stress that produced the discontinuity itself (shearing or tensile joints).

An important aspect that must be taken into account is the scale of observation: in fact, roughness of discontinuity walls can be characterized by a waviness (large scale undulation that can cause dilation during shear displacements) and by an unevenness (small scale roughness that tends to be damaged during shear displacements) [ISRM, 1978]. It is proven also that roughness varies with the dimension of the analyzed portion of surface [BARTON and CHOUBEY, 1977; FARDIN, 2008; TATONE and GRASSELLI, 2013]. In addition, the choice of the SI, required by the geometrical descriptors, influences the descriptors values [YU and VAYSSADE,1991; YANG *et al.*, 2001; JANG *et al.*, 2014]. In general by decreasing the SI roughness value increases: since roughness becomes stable below a certain interval, an optimal SI can be identified. This optimal value depends on the surface roughness: in particular, it decreases when roughness increases.

Moreover, discontinuity surfaces can be characterized by a geometrical anisotropy, namely, roughness evaluation is influenced by the measurement direction.

In conclusion, roughness is an uneven, anisotropic and size-dependent property of a discontinuity surface and these factors should be considered and analyzed during roughness measurement, in order to correctly estimate discontinuity shear strength.

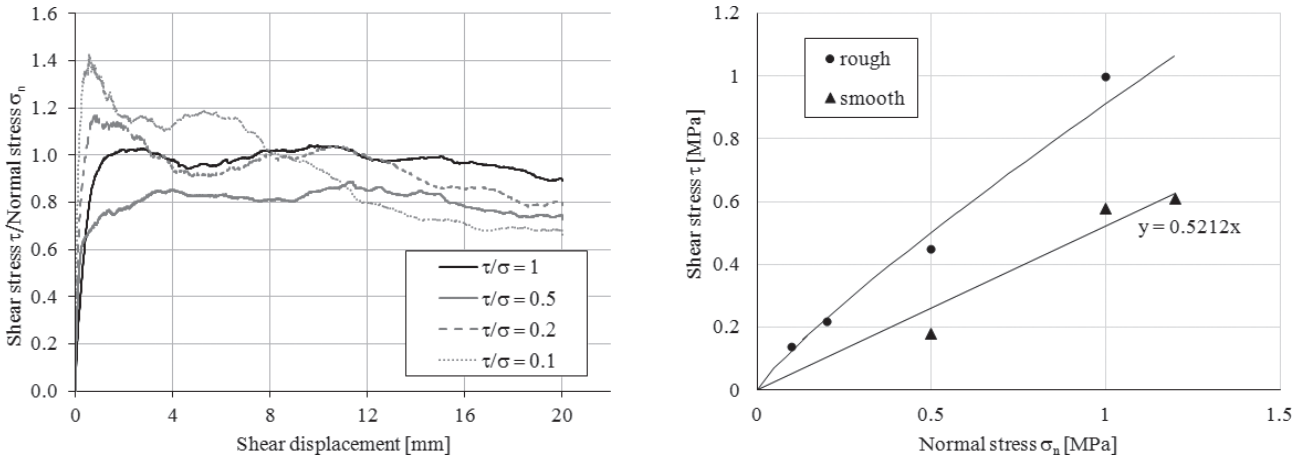

Fig. 1 – left) Stress-displacement curves obtained from monotonic shear tests; right) peak (on rough discontinuities) and residual (on smooth discontinuity) strength criteria

Fig. 1 – A sinistra) Curve tensione-spostamento ottenute dalle prove di taglio monotoniche; a destra) criteri di resistenza in condizioni di picco (su discontinuità rugosa) e residue (su discontinuità liscia)

Several authors [GENTIER *et al.*, 2000; BELEM *et al.*, 2000; TATONE and GRASSELLI, 2013] analyzed geometrical anisotropy of joints by considering 2D profiles extracted along different directions from a sampling surface. The anisotropy degree can be quantified by using the following equation [BELEM *et al.*, 2000], or its reciprocal [TATONE and GRASSELLI, 2013]

$$K_a = \frac{b}{a} = \frac{\min(p_x, p_y)}{\max(p_x, p_y)} \qquad (19)$$

where a and b represent the half–axes of the anisotropy ellipse along the x and y directions, respectively, and P_x and P_y the geometric parameters describing the discontinuity roughness calculated along the two axes.

Following equation 19, K_a can range between 0 (corresponding to surfaces with saw teeth, undulated surfaces, etc.) and 1 (isotropic surface).

YANG and LO [1997] proposed an index, the Hurst exponent H, which is based on the theory of fractional Brownian motion, to represent the anisotropy of joint roughness. The Hurst exponent can indicate the directional roughness for a profile according to the different sampling sequence.

7. Case study

7.1. Shear tests

The two tested specimens contain a side of a discontinuity each (80 mm x 80 mm). The specimens were artificially reproduced with mortar as replicas of the two sides of a real rock discontinuity [FERRERO *et al.*, 2010]. The mortar used is a high-performance water-based mortar having a nominal uniaxial compressive strength after 7 days - aging of 40 MPa. On these specimens and on smooth ones a series of monotonic and cyclic tests, with different normal stress values, was performed [FERRERO *et al.*, 2010]. From the test along smooth discontinuities a friction angle of 28° was found. The results of the tests carried out along rough discontinuities (Fig. 1a) were interpreted following Barton's criterion, by considering the smooth friction angle and a JCS of 40 MPa, which corresponds to the mortar compressive strength. From the best fitting Barton's curve (Fig. 1b) a JRC of 9.3 was obtained.

On each sample, a series of 16 markers were placed to force the reference system being the same in all the scans. The geometry of the joint was scanned before and after each test by means of a photogrammetric survey. A 105 mm lens mounted on a digital camera Nikon D100 was used for acquiring six images for each specimen; a photo restitution code based on structure from motion algorithm [HARTLEY and ZISSERMAN, 2000; RONCELLA *et al.*, 2005] was then run to produce a dense point cloud representing the joint surface. The estimated accuracy of the point coordinates is below 100 μm. Both the surfaces making up the discontinuity have been scanned: since they are positioned in the shear box along a vertical plane, they have been nominated right surface (S_R) and left surface (S_L), respectively.

7.2. Roughness analysis

In the following we will refer to the two original samples representing the sides (S_R and S_L) of a discontinuity, before any test. For both samples, a TIN (Triangular Irregular Network) was obtained, namely constituted by 3D points evenly scattered on the surface, with a density of about 9 pts/mm^2. Each

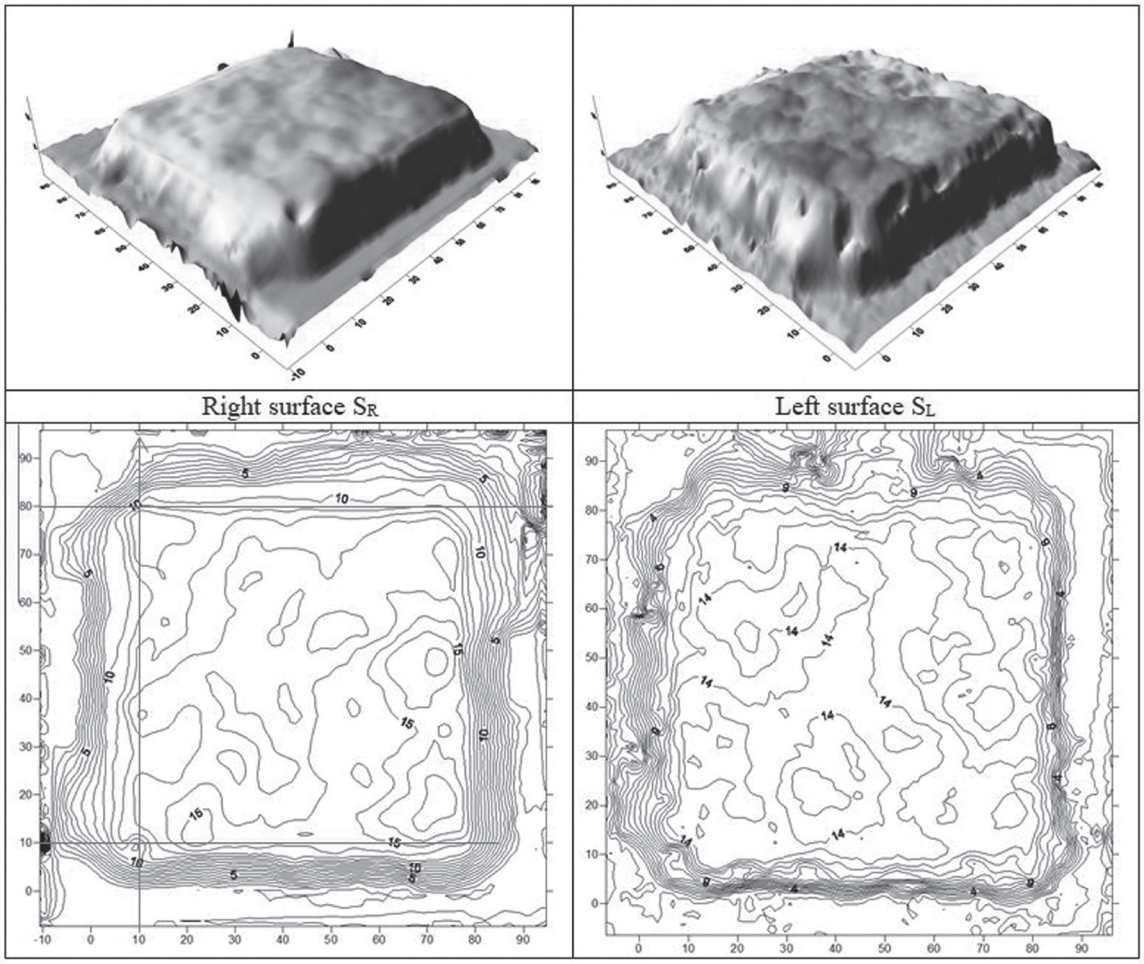

Fig. 2 – GRID and contour map of right and left surfaces of the considered joint.
Fig. 2 – Modello GRID e a curve di livello delle superfici destra e sinistra della discontinuità considerata.

TIN was input in Surfer (Golden Software Inc.) in order to convert it into a GRID (Fig. 2), namely a regular x-y grid in which the z coordinates are obtained from z values of the original TIN with a specific interpolation algorithm: among the available ones, we chose the first order polynomial regression, based on the relation $z(x,y) = A + Bx + Cy$; since the point density is pretty high (averagely 1 point every 0.33 mm) and the relation is linear, the influence of the interpolation method can be considered very low.

For each original point cloud, five GRIDs have been extracted, each of them having a constant spacing Δx of 1 mm along the x direction, and a different Δy spacing of 0.1, 0.2, 0.5, 1 e 2 mm, along the y-shear direction.

The x and y–profiles obtained from each GRID have been analyzed with the aim to compute the geometrical descriptors of the surface roughness directly obtainable by the profile (Z_2, θ^*_{max} - C and R_p) and the derived values of JRC computed by means of the empirical formulas above reported (Eqs. from 8 to 15).

This has allowed the authors to analyze the uneven distribution of the asperity on the discontinuity surface, to measure its anisotropic coefficient and to study the influence of the profile spacing on the roughness evaluation.

7.3. Asperity uneven distribution

65 profiles were extracted from S_R and S_L in both directions (x and y), considering GRIDs with a SI of 1 mm: the geometrical descriptors Z_2 (Eq. 2), JRC (Eqs. 8,10-13) and R_p (Eq. 4) were calculated for each profile. Results obtained for each surface and direction were statistically analyzed, in order to find simple and cumulative frequency distribution, minimum, maximum, median, mode and mean value and standard deviation (Tables 1 and 2). In Table 3 the simple and cumulative frequency distribution of the geometrical descriptors calculated along x and y direction of S_R and S_L are reported. It is possible to notice that whatever the descriptor, the variability of values is significant along the surface. For exam-

Tab. I – Statistical parameters describing the frequency distributions of the geometrical descriptors obtained on S_R along the x and y directions.

Tab. I – Parametri statistici che descrivono le distribuzioni di frequenza dei descrittori geometrici calcolati su S_R lungo le direzioni x e y.

S_R						
	Z_2 Eq. 2	JRC			Rp Eq. 4	
		Tse & Cruden Eq. 8	Yang, Lo, Di Eq. 10	Tatone & Grasselli Eq. 13		
min	0.148	10.3	5.3	6.1	1.011	Along Y direction
mean	0.198	14.2	9.3	9.2	1.019	
max	0.305	20.4	15.7	15.0	1.041	
standard deviation	0.037	2.4	2.5	2.1	0.007	
median	0.183	13.3	8.4	8.4	1.016	
mode	0.180	13.0	8.0	8.0	1.016	
min	0.200	14.5	9.6	9.4	1.019	Along X direction
mean	0.275	18.8	14.0	13.4	1.033	
max	0.405	24.4	19.7	19.8	1.061	
standard deviation	0.051	2.5	2.6	2.6	0.010	
median	0.261	18.2	13.4	12.8	1.030	
mode	0.260	18.0	14.0	13.0	1.031	

Tab. II – Statistical parameters describing the frequency distributions of the geometrical descriptors obtained on S_L along the x and y directions.

Tab. II – Parametri statistici che descrivono le distribuzioni di frequenza dei descrittori geometrici calcolati su S_L lungo le direzioni x e y.

S_L						
	Z_2 Eq. 2	JRC			Rp Eq. 4	
		Tse & Cruden Eq. 8	Yang, Lo, Di Eq. 10	Tatone & Grasselli Eq. 13		
min	0.139	9.4	4.4	5.5	1.010	Along Y direction
mean	0.179	12.8	7.9	8.1	1.016	
max	0.314	20.9	16.1	15.5	1.043	
standard deviation	0.029	2.1	2.1	1.7	0.005	
median	0.173	12.5	7.6	7.8	1.014	
mode	0.180	12.71	7.82	7.9	1.016	
min	0.115	6.7	1.8	3.8	1.007	Along X direction
mean	0.167	11.7	6.8	7.3	1.014	
max	0.284	19.4	14.7	14.0	1.036	
standard deviation	0.029	2.4	2.4	1.8	0.005	
median	0.165	11.8	6.8	7.2	1.013	
mode	0.181	18.0	8.45	8.4	1.031	

ple, considering y direction along both the S_R and S_L surfaces, the most frequent class of JRC is 8 and this agrees with JRC value (equal to 9.2) obtained from the back-analysis of laboratory tests. Y direction corresponds to the shearing direction imposed during the laboratory test.

7.4. Anisotropy

Regarding anisotropy, results obtained along x and y considering a SI of 1 mm have been compared: anisotropy was calculated by means of equation 19, where P_x and P_y represent the average values of the geometrical parameters obtained along the x and y direction respectively. In Table 4 the anisotropy values are reported: it is possible to point out that S_R evidences a higher degree of anisotropy (Ka ~ 0.6-0.7), while S_L can be considered as isotropic (Ka ~ 0.9).

7.5. Influence of SI

The influence of the profile SI was investigated by analyzing y profiles of S_R belonging to the different created GRIDs (SI equal to 0.1, 0.2, 0.5, 1 and 2

Tab. III – Frequency distribution and cumulative frequency of Z_2 (Eq. 2), JRC (Eq. 13) and (Rp-1) (Eq. 4) along x and y directions of S_R and S_L.

Tab. III – Distribuzione di frequenza e frequenza cumulata di Z_2 (Eq. 2), JRC (Eq. 13) e (Rp-1) (Eq. 4) lungo le direzioni x e y di S_R e S_L.

	S_R	S_L
Z_2	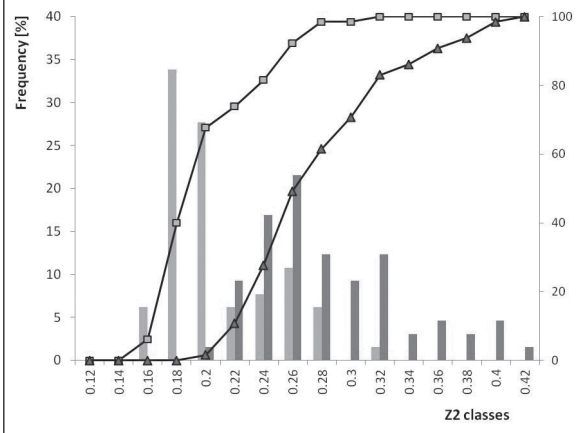	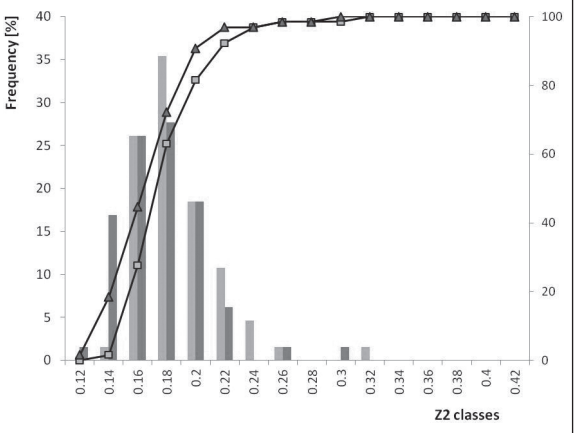
JRC	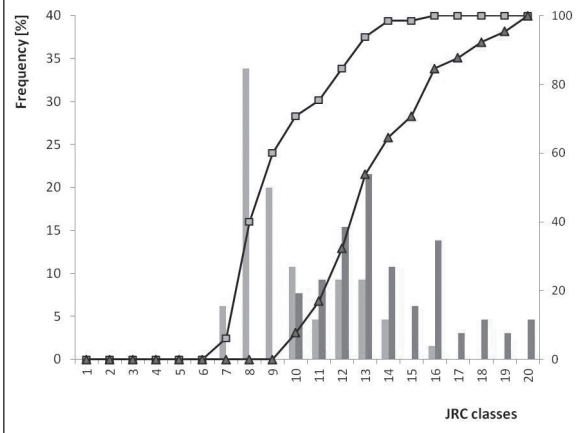	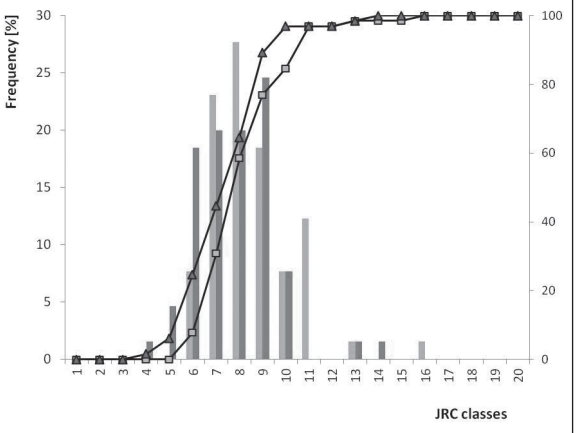
Rp-1	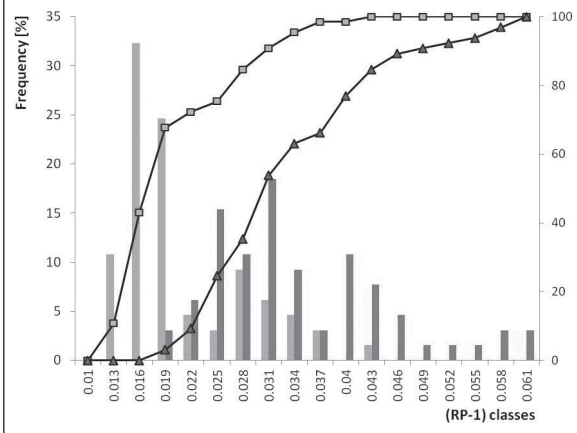	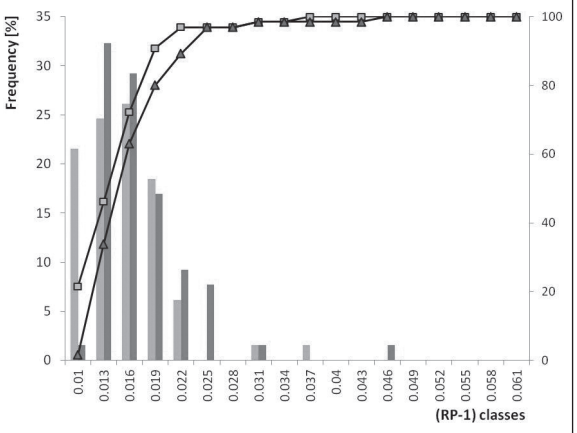
	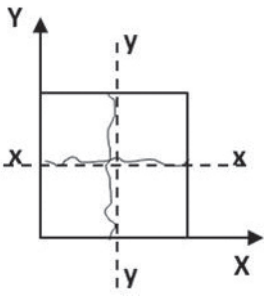	

Tab. IV – Anisotropy values.
Tab. IV – Valori di anisotropia.

Surface	Z_2 Eq. 2	JRC Tse & Cruden Eq. 8	JRC Yang, Lo, Di Eq. 10	JRC Tatone & Grasselli Eq. 13	(Rp-1) Eq. 4
S_R	0.72	0.76	0.67	0.69	0.58
S_L	0.93	0.92	0.87	0.90	0.87

Tab. V – Values of Z_2 computed for the y-profiles of S_R with different SI and derived JRC values following equations 8-13.
Tab. V – Valori di Z_2 calcolati per i profili lungo la direzione y di S_R con diversi passi di analisi e relativi valori di JRC ottenuti mediante equazioni 8-13.

	Z2			JRC														
SI [mm]	Eq. 2			Tse & Cruden (Z_2) Eq. 8			Tse & Cruden (SF) Eq. 9			Yang, Lo, Di (Z_2) Eq. 10			Yang, Lo, Di (SF) Eq. 11			Tatone & Grasselli Eq. 13		
	Av.	max	min	Av.	Max	min	Av.	max	min	Av.	max	min	Av.	max	min	Av.	max	min
2	0.19	0.29	0.14	13.7	19.9	9.8	13.3	19.6	9.3	8.9	15.1	4.9	15.2	21.1	11.5	8.9	14.5	5.8
1	0.20	0.30	0.15	14.2	20.4	10.3	13.8	20.2	9.8	9.3	15.7	5.3	15.6	21.6	11.9	9.2	15.0	6.1
0.5	0.20	0.31	0.15	14.3	20.6	10.4	13.9	20.3	9.9	9.4	15.9	5.5	15.8	21.8	12.1	9.3	15.2	6.2
0.2	0.20	0.31	0.15	14.4	20.8	10.5	14.0	20.5	10.0	9.5	16.0	5.6	15.9	22.0	12.2	9.4	15.4	6.3
0.1	0.20	0.32	0.15	14.6	21.1	10.5	14.2	20.9	10.4	9.7	16.4	6.0	16.0	22.3	12.5	9.6	15.8	6.6

Table VI – Values of θ*max - C parameters (Eq. 6) for the y-profile, along positive and negative ways, of SR with different SI and derived JRC values (Eq. 15).
*Tabella VI – Valori dei parametri θ*max - C (Eq. 6) per i profili lungo la direzione y di SR, con verso positivo e negativo, con diversi passi di analisi e relativi valori di JRC (Eq.15).*

	Positive direction									Negative direction								
SI [mm]	θ_{max} [°] Eq. 6			C [] Eq. 6			JRC Eq. 15			θ_{max} [°] Eq. 6			C [] Eq. 6			JRC Eq. 15		
	Av.	max	min	Av.	Max	min	Av.	max	min	Av.	max	min	Av.	max	min	Av.	max	min
2	17.3	42.7	7.7	1.9	3.3	0.6	6.6	12.3	4.8	33.8	43.1	24.7	3.00	3.00	3.00	10.3	13.7	6.9
1	21.0	47.5	10.6	2.3	4.4	1.0	7.1	10.7	5.6	34.6	49.9	25.2	3.18	5.24	1.71	10.1	9.6	11.6
0.5	23.2	49.7	11.5	2.6	5.0	1.1	6.5	9.5	5.2	35.7	53.8	26.0	3.30	5.18	1.70	9.4	10.0	11.3
0.2	25.2	54.0	11.9	2.9	5.3	1.2	6.5	9.8	5.0	37.1	56.5	26.8	3.41	5.87	1.83	9.5	9.3	11.1
0.1	27.5	57.1	12.4	3.2	5.6	1.4	6.6	9.9	4.6	39.3	58.5	29.2	3.61	6.09	2.33	9.7	9.3	10.1

mm). Values of Z_2 (Eq. 2), θ^*_{max} and C (Eq. 6) along positive and negative direction (defined by the authors) and the derived JRC values (Eqs. 8,9,10,11,13) were calculated: Tables 5 and 6 rep[illegible]hem. Figures 3 and 4 show mean values of (θ^*_{max} C) and Z_2, respectively, obtained by varying the SI. It is possible to observe that both θ^*_{max} and C decrease significantly by increasing the SI. Moreover, roughness is different along positive and negative direction: in particular, in this case it is greater along the negative one. This fact was already pointed out by the authors [FERRERO *et al.*, 2010] in light of the results of cyclic tests performed on the same samples, which highlighted an asymmetric behavior regarding joint shear strength

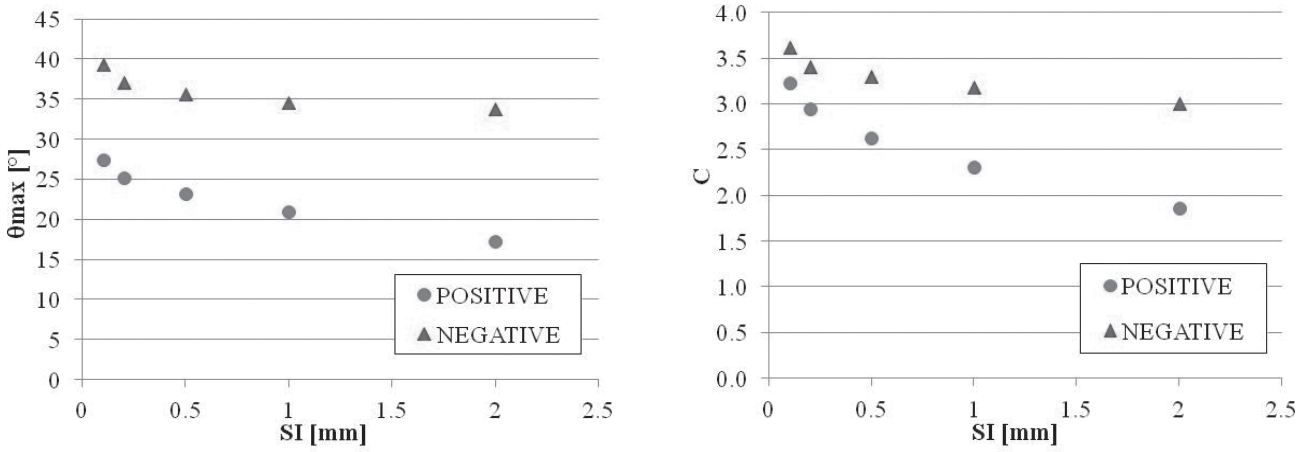

Fig. 3 – Tatone and Grasselli's roughness parameters θ^*_{max} and C vs SI.
Fig. 3 – Parametri di rugosità θ^*_{max} e C proposti da Tatone e Grasselli in funzione del passo di analisi.

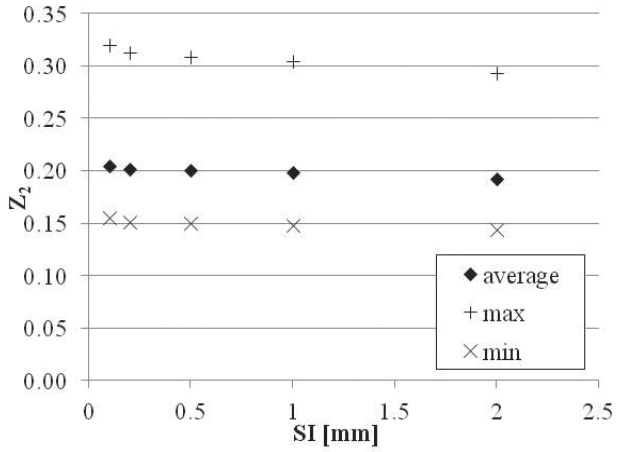

Fig. 4 – Z_2 vs SI
Fig. 4 – Z_2 in funzione del passo di analisi

along the two considered directions. Similarly, Z_2 decreases by increasing the SI (Fig. 4). Figure 5 shows mean values of JRC calculated from SF, Z_2 and (θ^*_{max}, C) by means of equations 8,9,10,11,13,15 and JRC values obtained from the back-analysis of laboratory tests. It is possible to observe that JRC increases by decreasing the SI and is extremely variable depending on the equation used.

Conclusions

In this paper the state of the art of the roughness descriptors is presented. The two surfaces composing a rock specimen subject to shear testing have been analyzed with the aim to compute the geometrical descriptors of the surface roughness directly obtainable by the profiles (Z_2, θ^*_{max} - C and R_p) and the derived values of JRC computed by means of empirical formulas (Eqs. from 8 to 15).

This has allowed the authors to analyze the uneven distribution of the asperity on the discontinuity surface, to measure its anisotropic coefficient and to study the influence of the SI on the roughness evaluation.

65 profiles were analyzed to find simple and cumulative frequency distribution, minimum, maximum, median, mode and mean value and standard deviation. It is possible to notice that whatever the descriptor, the variability of values is significant along the surface.

Regarding anisotropy, all applied formulas are able to quantify this aspect and it is possible to point out that the two surfaces of the joint show different levels of anisotropy: S_R evidences a higher degree of anisotropy (Ka ~ 0.6-0.7), while S_L can be considered as isotropic (Ka ~ 0.9).

It has also been shown that sampling interval has a great influence on the geometrical descriptor determination: JRC increases by decreasing the SI, even if it is extremely variable depending on the equation used. A similar variability can be observed along S_L and along x direction of both surfaces.

The comparison between values of JRC calculated from SF, Z_2 and (θ^*_{max}, C) by means of equations 8-9-10-11-13-15 and JRC values obtained from the back-analysis of laboratory tests show as Tatone and Grasselli's formulation gives the best agreement when considering the most rough part of the sample. In conclusion, the possibility offered by digital surface models to evaluate roughness by means of quantitative geometrical descriptors allows for a quick and complete investigation of whole discontinuity surfaces.

Whilst the great amount of data obtainable from this kind of analysis allows for a statistical evaluation of roughness variability, on the other hand it underlines the complexity of the description of roughness nature and effects on shear strength by means of a single value of JRC.

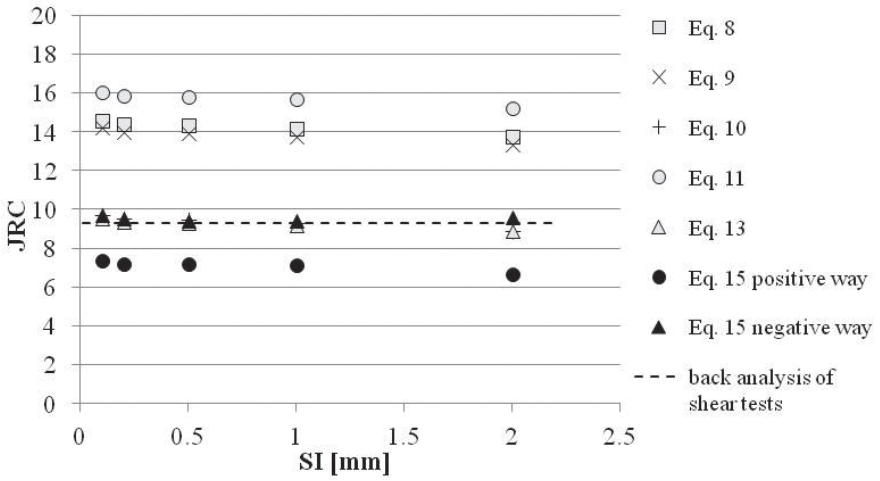

Fig. 5 – JRC derived from Z_2 and θ^*_{max} - C parameters vs SI
Fig. 5 – JRC ottenuto mediante correlazioni con i parametri Z_2 e θ^*_{max} - C in funzione del passo di analisi

References

BARTON N. (1973) – *Review of a new shear strength criterion for rock joints.* Engineering Geology, 7, n. 4, pp. 287-332.

BARTON N. (1976) – *Shear strength of rock and rock joints.* International Journal of Rock Mechanics and Mining Sciences & Geomechanics Abstracts, 13, n. 9, pp. 255-279.

BARTON N., CHOUBEY V. (1977) – *The shear strength of rock joints in theory and practice.* Rock Mechanics and Rock Engineering, 10, [illegible]2, pp. 1-54.

BELEM T., HOMAND-ETIENNE F., SOULEY M. (2000) – *Quantitative parameters for rock joint surface roughness.* Rock Mechanics and Rock Engineering, 33, n. 4, pp. 217-242.

BELEM T., HOMAND-ETIENNE F., SOULEY M. (1997) – *Fractal analysis of shear joint roughness.* International Journal of Rock Mechanics & Mining Sciences, 34, [illegible]-4, paper n.. 130.

[illegible] J.R. (1990) – *Repair, Evaluation, Maintenance and Rehabilitation Research Program. Surface Roughness Characterization of Rock Masses Using the Fractal Dimension and the Variogram* (No. WES/TR/GL-REMR-GT-14). [illegible]MY ENGINEER WATERWAYS EXPERIMENT [illegible]TION VICKSBURG MS GEOTECHNICAL LAB.

CHEN S.J., ZHU W.C., YU Q.L., LIU X.G. (2016) – *Characterization of anisotropy of joint surface roughness and aperture by variogram approach based on digital image processing technique.* Rock Mechanics and Rock Engineering, 49, n. 3, pp. 855-876.

EL-SOUDANI SM. (1978) – *Profilometric analysis of fractures.* Metallography, 11, n. 3, pp. 247-336.

FARDIN N. (2008) – *Influence of structural non-stationarity of surface roughness on morphological characterization and mechanical deformation of rock joints.* Rock Mechanics and Rock Engineering, 41, n. 2, pp. 267-297.

FARDIN N., STEPHANSSON O., JING L. (2001) – *The scale dependence of rock joint surface roughness.* International Journal of Rock Mechanics & Mining Sciences, 38, n. 5, pp. 659-669.

FERRERO A.M., GIANI G.P. (1990) – *Geostatistical description of the joint surface roughness.* In: Paper in Rock Mechanics Contributions and Challenges: Proceedings of the 31st [illegible]S Symposium, [illegible]ed by WA Hustrulid and GA Joh[illegible]n, CO Sch. Mines, Golden, CO, pp. 463-470.

FERRERO A.M., MIGLIAZZA R., TEBALDI G. (2010) – *Development of a New Experimental Apparatus for the Study of the Mechanical Behaviour of a Rock Discontinuity Under Monotonic and Cyclic Loads.* Rock Mechanics and Rock Engineering 43, n. 6, pp. 685-695.

GE Y., KULATILAKE P.H.S.W., TANG H., XIONG C. (2014) – *Investigation of natural rock joint roughness.* Computers and Geotechnics, 55, pp. 290-305.

GENTIER S., RISS J., ARCHAMBAULT G., FLAMAND R., HOPKINS D. (2000) – *Influence of fracture geometry on shear behaviour.* International Journal of Rock Mechanics & Mining Sciences, 37, n. 1-2, pp. 161-174.

GIANI G.P. (1992) – *Rock slope stability analysis.* Rotterdam: A.A Balkema Publishers.

GRASSELLI G., WIRTH J., EGGER P. (2002) – *Quantitative three-dimensional description of a rough surface and parameter evolution with shearing.* International Journal of Rock Mechanics & Mining Sciences, 39, n. 6, pp. 789-800.

HARTLEY R., ZISSERMAN A. (2000) – *Multiple View Geometry in computer vision.* Cambridge University Press, Cambridge.

MURALHA J., GRASSELLI G., TATONE B., BLÜMEL M., CHRYSSANTHAKIS P., YUJING J. (2014) – *ISRM Suggested Method for Laboratory Determination of the Shear Strength of Rock Joints: Revised Version.* Rock Mechanics and Rock Engineering, 47, n. 1, pp. 291-302.

ISRM (1978) – *Commission on standardization of laboratory and field tests. Suggested methods for the quantitative description of discontinuities in rock masses.* International Journal of Rock Mechanics and Mining Sciences & Geomechanics Abstracts, 15, n. 6, pp. 319-368.

JANG H.S., KANG S.S., JANG B.A. (2014) – *Determination of Joint Roughness Coefficients Using Roughness Parameters.* Rock Mechanics and Rock Engineering 47, n. 6, pp. 2061-2073.

JIANG Y., LI B., TANABASHI Y. (2006) – *Estimating the relation between surface roughness and mechanical properties of rock joints.* International Journal of Rock Mechanics & Mining Sciences 43, n. 6, pp. 837-846.

JOURNEL A.G., HUIJBREGTS CH.J. (1978). *Mining geostatistics*, London, Academic Press.

KULATILAKE P.H.S.W., UM J. (1997) – *Requirements for accurate quantification of self affine roughness using the roughness-length method.* International Journal of Rock Mechanics & Mining Sciences, 34, n. 3-4, p. 166.e1 – 166.e15.

KULATILAKE P.H.S.W., UM J., PAN G. (1998) – *Requirements for accurate quantification of self-affine roughness using the variogram method.* International Journal of Solids And Structures, 35, nn. 31-32, pp. 4167-4189.

LI Y., HUANG R. (2015) – *Relationship between joint roughness coefficient and fractal dimension of rock fracture surfaces.* International Journal of Rock Mechanics & Mining Sciences, 75, pp. 15-22.

LI Y., ZHANG Y. (2015) – *Quantitative estimation of joint roughness coefficient using statistical parameters.* International Journal of Rock Mechanics & Mining Sciences, 77, pp. 27-35.

MAERZ N.H., FRANKLIN J.A., BENNETT C.P. (1990) – *Joint roughness measurement using shadow profilometry.* International Journal of Rock Mechanics and Mining Sciences & Geomechanics Abstracts, 27, n. 5, pp. 329-343.

MANDELBROT B.B. (1983) – *The fractal geometry of nature.* Freeman, San Francisco.

MANDELBROT B.B. (1985) – *Self-affine fractals and fractal dimension.* Physica Scripta, 32, n. 4, pp. 257-260.

MANDL G. (2005) – *Rock Joints: The Mechanical Genesis.* Springer Berlin Heidelberg.

MYERS N.O. (1962) – *Characterization of surface roughness.* Wear, 5, pp. 182-189.

ODLING N.E. (1994) – *Natural fracture profiles, fractal dimension and joint roughness coefficients.* Rock Mechanics and Rock Engineering, 27, n. 3, pp. 135-153.

ROKO R.O., DAEMENJ J.J.K., MYERS D.E. (1997) – *Variogram characterization of joint surface morphology and asperity deformation during shearing.* International Journal of Rock Mechanics & Mining Sciences, 34, n. 1, pp. 71-84.

RONCELLA R., FORLANI G., REMONDINO F. (2005) – *Photogrammetry for geological applications: automatic retrieval of discontinuity orientation in rock slopes.* In: Videometrics IX, electronic imaging, IS&T/SPIE 17th Annual Symposium, pp 17-27.

SAYLES R.S., THOMAS R.R. (1977) – *The spatial representation of surface roughness by means of the structure functions, a practical alternative to correlation.* Wear, 42, pp. 263-276.

TATONE B.S.A., GRASSELLI G. (2013) – *An investigation of discontinuity roughness scale dependency using high-resolution surface measurements.* Rock Mechanics and Rock Engineering, 46, n. 4, pp. 657-681.

TATONE B.S.A., GRASSELLI G. (2010) – *A new 2D discontinuity roughness parameter and its correlation with JRC.* International Journal of Rock Mechanics & Mining Sciences, 47, n. 8, pp. 1391-1400.

TSE R., CRUDEN D.M. (1979) – *Estimating joint roughness coefficients.* International Journal of Rock Mechanics and Mining Sciences & Geomechanics Abstracts,16, pp. 303-307.

YANG Z.Y., LO S.C., DI C.C. (2001) – *Reassessing the joint roughness coefficient (JRC) estimation using Z_2.* Rock Mechanics and Rock Engineering, 34, n. 3, pp. 243-251.

YANG Z.Y., LO S.C. (1997) – *An index for describing the anisotropy of joint surfaces.* International Journal of Rock Mechanics & Mining Sciences, 34, n. 6, pp. 1031-1044.

YU X., VAYSSADE B. (1991) – *Joint profiles and their roughness parameters.* International Journal of Rock Mechanics & Mining Sciences & Geomechanics Abstracts, 28, n. 4, pp. 333-336.

Confronto tra metodi per la stima della rugosità delle discontinuità

Sommario

Gli ammassi rocciosi sono mezzi naturali nei quali la presenza di discontinuità influenza significativamente le condizioni di stabilità: i blocchi sono generati dai piani di discontinuità e possono mobilitarsi lungo di essi; inoltre, i possibili cinematismi sono governati dalla quantità di resistenza a taglio offerta dalle discontinuità. La resistenza a taglio di una discontinuità dipende dalle sue proprietà meccaniche ma anche dagli aspetti geometrici, come la sua rugosità. Per questa ragione, la quantificazione di questa proprietà è fondamentale. In questo lavoro è presentato lo stato dell'arte inerente i descrittori della rugosità. Le due superfici di una discontinuità, digitalizzate mediante rilievo fotogrammetrico e precedentemente utilizzate per effettuare prove di taglio [FERRERO et al., 2010], sono utilizzate per applicare i descrittori geometrici ed analizzare i risultati in termini di corrispondenza con i risultati di laboratorio. Inoltre, viene discussa l'influenza dell'anisotropia e del passo di campionamento. Questo lavoro confronta diversi descrittori quantitativi della rugosità, mostrando come l'approccio di TATONE e GRASSELLI [2011; 2013] sia in buon accordo con i risultati sperimentali delle prove di taglio.